

# Multiparticle Computer Simulation of Photosynthetic Electron Transport in the Thylakoid Membrane

I. B. Kovalenko<sup>a</sup>, A. M. Abaturova<sup>a</sup>, D. M. Ustinin<sup>a</sup>,  
G. Yu. Riznichenko<sup>a</sup>, E. A. Grachev<sup>b</sup>, and A. B. Rubin<sup>a</sup>

<sup>a</sup>Biological Faculty, Moscow State University, Moscow, 119992 Russia

<sup>b</sup>Physical Faculty, Moscow State University, Moscow, 119992 Russia

Received November 3, 2006; in final form, November 21, 2007

**Abstract**—Further developing the method for direct multiparticle modeling of electron transport in the thylakoid membrane, here we examine the influence of the shape of the reaction volume on the kinetics of the interaction of the mobile carrier with the membrane complex. Applied to cyclic electron transport around photosystem I, with account of the distribution of complexes in the membrane and restricted diffusion of the reactants, the model demonstrates that the biphasic character of the dark reduction of P700<sup>+</sup> is quite naturally explained by the spatial heterogeneity of the system.

**DOI:** 10.1134/S0006350907050053

*Key words:* photosystem I, cyclic electron transport, kinetic modeling, direct simulation modeling, lateral diffusion

## THE NECESSITY OF DIRECT MODELING OF ELECTRON TRANSPORT IN THE PHOTOSYNTHETIC MEMBRANE

In green plants and algae, the delivery of a light energy quantum to the photosynthetic reaction center initiates charge separation and electron transport along a chain of carriers. The latter process comprises basically different steps: electron transfer within multisubunit membrane complexes (PS I, PS II, and cyt *b<sub>6</sub>f*); electron transport by mobile carriers (Fd, Pc, PQ); and interactions between such partners. The complexes are imbedded in the membrane, and their distribution is not random. The thylakoid membrane is elaborately organized in space, forming a network of membrane cylindrical stacks (grana) and interconnecting stroma lamellae with a common continuous lumen (see, e.g., [1]). The granal membrane regions contain PS II complexes; the regions protruding into

the stroma carry PS I; the *bf* complex is dispersed throughout the membrane.

Each mobile carrier can move within its compartment: Fd in the stroma, Pc in the lumen, and PQ in the membrane lipid layer. The Pc molecules oxidize the *bf* complex and reduce the PS I reaction center, traveling in the luminal space over quite large distances (hundreds of nanometers) to transport electrons between the granal and the stromal regions in the thylakoid [2–4]; this is supposed to take place by light-driven diffusion [5]. However, the total span of the lumen (4–10 nm [6]) is commensurate with the size of the Pc molecule; considering also the protruding parts of numerous transmembrane complexes [7, 8], such environs can hardly provide for free diffusion.

Plastoquinone has to diffuse within the membrane where more than half of the volume is occupied by transmembrane proteins [9]. Analysis of PQ movement in a membrane uniformly filled with complexes [10] suggested the existence of protein-limited diffusional microdomains: the PQ diffusion rate is high

**Abbreviations:** CET, cyclic electron transport; Fd, ferredoxin; FNR, ferredoxin:NADP<sup>+</sup> oxidoreductase; FQR, ferredoxin:quinone oxidoreductase; Pc, plastocyanin; PQ, plastoquinone; PS, photosystem.

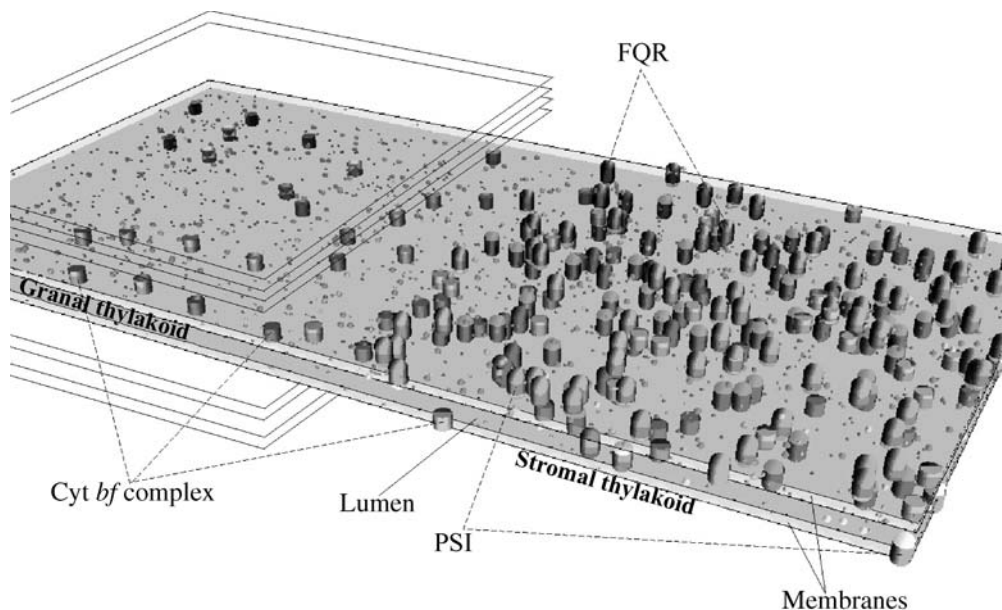


Fig. 1. The stage of the multiparticle direct model.

within one such microdomain, but a much longer time is needed for transit to another one.

Although Fd molecules generally diffuse in a relatively large aqueous space (stroma), their diffusion in the most functionally essential region—near the thylakoid membrane—may also be hindered by the protuberances of multiple protein complexes.

Thus, for all mobile carriers a routine description of electron transport with chemical kinetic equations is inadequate to the contemporary notions on the architectonics of the photosynthetic system. It is necessary to consider the Brownian motion of mobile carriers in a heterogeneous medium.

Indeed, the conventional kinetic models are based on the apparatus of ordinary differential equations, using the law of mass action to describe the reaction between a mobile carrier and a complex and the state probability equations to describe electron transfer within the complex [11–14], while the process of carrier diffusion itself is not considered directly. Such models cannot take into account the intricate spatial organization of the thylakoid system and the nonuniform distribution of the membrane complexes. A mathematical model constructed with regard for the lateral heterogeneity of thylakoids [15] still cannot describe local fluctuations in the mobile carrier and proton concentrations or restricted diffusion of the carriers in the lumen and within the membrane.

Models based on Brownian dynamics afford detailed description of one mobile carrier and its binding with a multisubunit enzyme complex [16–20]; however, this method is inapplicable to processes involving multiple intramembrane complexes, mobile carriers, and obstacles for diffusion.

Hence, modeling of subcellular processes with account of the details of their spatial and functional organization requires novel approaches whereby the physical and biological notions on particular steps can be integrated in a unified computable model. Such direct, multiparticle simulation models can incorporate various formalisms for describing separate events with different kinetic mechanisms.

We have previously outlined a direct multiparticle model of electron transport processes in the thylakoid membrane [21, 22]. Here we further this approach, assessing the influence of the shape of the reaction volume on the kinetics of interaction between two proteins, estimating the model parameters, and testing the model in simulating cyclic electron transport.

## MODEL DESCRIPTION

Our multiparticle model is compartmental and can be envisaged as a 3D stage comprising the thylakoid membrane, the lumen, and the stromal space (Fig. 1). The algorithm generating the stage has been described elsewhere [23]. The motion of Pc, Fd,

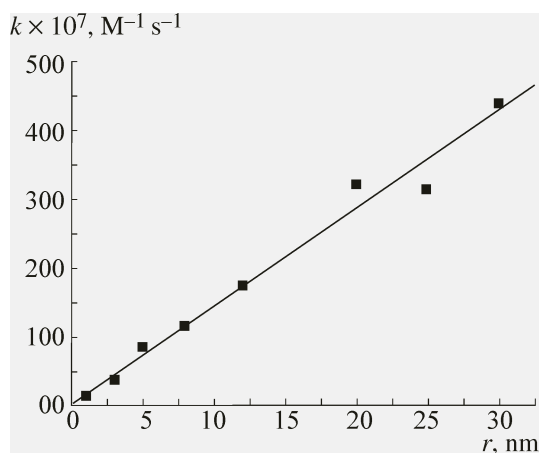


**Fig. 2.** Dependence of the rate constant for the bimolecular D–A reaction on the effective interaction radius at docking probability  $p = 1$ ;  $k$  obtained by fitting the direct model curve with Eq. (1).

and PQ in their respective compartments is modeled using the mathematical formalism of Brownian motion with account of the geometrical constraints imposed by the organization of the model stage; at every step the direction can change at random and the velocity obeys a normal distribution.

Basically, one may discern four steps in an overall redox reaction between two proteins in solution: (1) Brownian diffusion; (2) mutual approach owing to electrostatic attraction and orientation in a preliminary complex; (3) formation of the transfer-competent complex (docking); (3) transfer of the electron within this ensemble. Here we consider the first step as the rate-limiting one; the other steps are taken into account implicitly with model parameters. Previously, steps 1 and 2 for the complexing of Pc and cyt  $f$  were examined in more detail [24].

In the direct model, it is assumed that if chaotic movement of the carrier brings it to the protein complex within a certain distance (effective interaction radius), the carrier binds thereto with a certain probability. The model allows for direct and back reactions of binding and electron transfer.

The behavior of a direct model is determined by a set of parameters such as diffusion coefficients for mobile carriers, docking probabilities, effective interaction radii, characteristic times of electron transfer. Thereby we obtain a time dependence of the redox state of each carrier, i.e., a kinetic curve, which can be characterized by amplitude and rate constant (changing with variation of the model parameters) and tested for the goodness of fit.

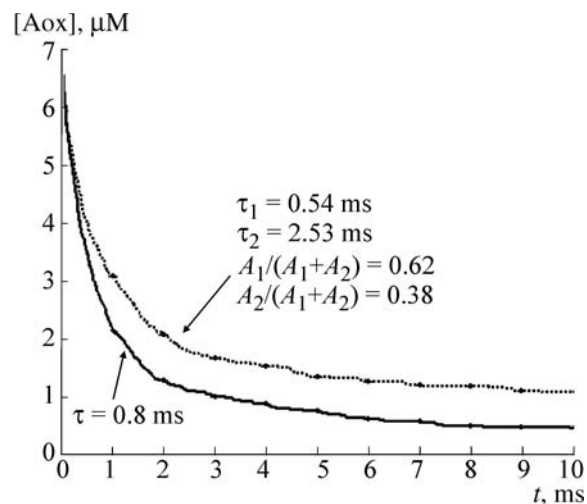
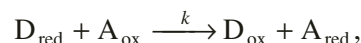


**Fig. 3.** Bimolecular reaction kinetics in the same volume of different shape. Broad gray lines represent the numerical experiments for (bottom) a cube and (top) a parallelepiped with a height/width ratio of about 1:100. The thin black line is the approximation of the kinetic curve (1) for the reaction in bulk.

#### ROLE OF THE SHAPE OF THE REACTION VOLUME

The direct model was used to examine how the kinetics of a redox reaction between a donor D and acceptor A in solution depends on the model parameters: interaction radius and docking probability. It was assumed that either molecule exists in two states, indexed (ox) and (red). The system was taken to be a cube of  $125 \cdot 10^6 \text{ nm}^3$ , with 500 molecules each of D and A, at the initial moment containing only  $D_{\text{red}}$  and  $A_{\text{ox}}$ .

For the reaction studied,



the curve of the redox state of A obtained in the direct model was characterized kinetically, with the rate constant  $k$ . In the kinetic approach the reaction is described by an ordinary differential equation

$$\frac{d[A_{\text{ox}}]}{dt} = -k[D_{\text{red}}][A_{\text{ox}}].$$

At the initial conditions, it is solved as

$$[A_{\text{ox}}](t) = \frac{D_{\text{red}}^0}{kD_{\text{red}}^0 t + 1} \quad (1)$$

where  $D_{\text{red}}^0$  is the initial concentration of reduced donor. To find the second-order reaction rate constant, the kinetic curves obtained with the multiparticle model were fitted with Eq. (1).

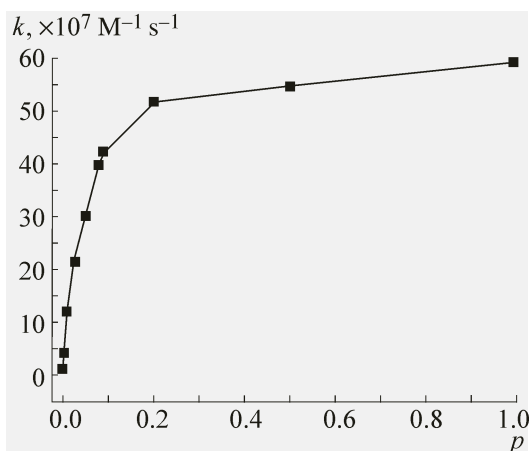


**Fig. 4.** Dependence of the rate constant for the bimolecular D–A reaction on the docking probability at an effective interaction radius  $r = 4$  nm;  $k$  obtained by fitting the direct model curve with Eq. (1).

Assessing the dependence of  $k$  on the effective interaction radius  $r$ , the docking probability was taken to be 1, i.e., molecules reacted in every approach; electron transfer was assumed to be rapid compared with diffusion.

The result of modeling is shown in Fig. 2. One can see that the rate of the bimolecular reaction linearly depends on  $r$ , which is in accord with the Smoluchowski equation for the steady-state rate of a diffusion-controlled reaction [25]. Here it appears as

$$v = 4\pi N_A r (D_D + D_A) c_D d_A, \quad (2)$$

where  $N_A$  is the Avogadro number,  $c$  are the concentrations and  $D$  are the diffusion coefficients. The Smoluchowski equation represents the law of mass action: the rate of a bimolecular reaction in solution depends linearly on the product of concentrations; is the second-order reaction rate constant proportional to the interaction radius.

The theoretical  $k$  values approximately correspond to those obtained in the numerical experiment with the direct model. The discrepancy appears because Eq. (2) assumes that  $r$  is small relative to the average intermolecular distance, while this is not always true in the multiparticle model. However, such modeling also shows that the reaction rate is proportional to D and A concentrations, just as it should be.

Then, we changed the dimensions of the reaction volume to a square-base parallelepiped of the same volume. The interaction radius was set at 4 nm. Numerical experiments with a docking probability about unity revealed that when the mean path traveled by a

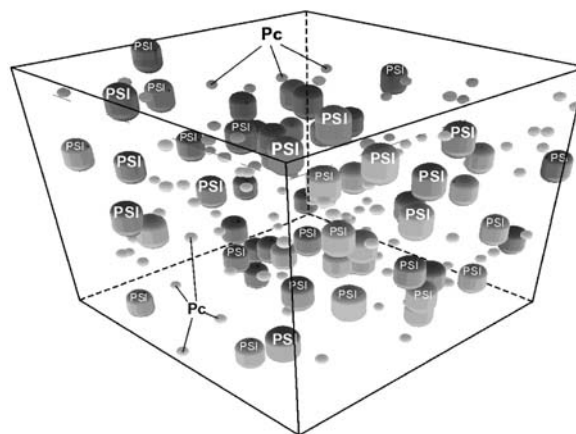


**Fig. 5.** Model of interaction of isolated carrier particles in solution (exemplified with PSI and Pc, not to scale).

Brownian particle to a reactive collision becomes comparable to the average distance between particles in solution, the law of mass action fails to adequately describe the kinetics of the reaction. Thus for a 500-nm cube the acceptor reduction curve is nicely approximated by Eq. (1), and  $k = 4.2 \cdot 10^8 \text{ M}^{-1} \text{ s}^{-1}$  (Fig. 3, lower curve). The shape of the curve and the rate constant remain the same as the height of the system is gradually reduced down to 100 nm at constant volume. However, further height reduction gives rise to significant discrepancies, and in, e.g., a system measuring  $2235 \times 2235 \times 25$  nm the model curve and the one calculated with (2) do not coincide at any  $k$  value (Fig. 3, upper curve). Indeed, the Smoluchowski equation was derived for reactions in bulk, whereas such a model system is closer to a two-dimensional case characteristic of a reaction in a membrane; kinetics of the latter is known to differ from that in solution [26].

We also examined the dependence of the rate constant on the docking probability, with D and A homogeneously distributed ( $0.2 \mu\text{M}$ ) in the cubic volume,  $r = 4$  nm, and diffusion coefficients of  $10^{-12} \text{ m}^2/\text{s}$ . The resulting curve (Fig. 4) shows expected proportionality at low  $p$  and tends to a plateau.

#### ESTIMATION OF MODEL PARAMETERS FOR ISOLATED PARTICLES IN SOLUTION

An important point in direct modeling is to estimate the model parameters from experimental data that are conventionally interpreted in the framework

of kinetic models. Some of these (e.g., concentration or distribution of complexes in the membrane) can be determined (by electron and atomic force microscopy). Others (e.g., docking probabilities and effective interaction radii) can be estimated from their influence on the kinetic constants for interaction of mobile and membrane carriers. Let us consider an example of Pc and PSI; parameters for PSI and Fd, *bf* and Pc were determined in the same way.

There are some works [7, 27, 28] on the interaction of Pc with the PSI reaction center P700. When electron transfer between Pc and P700<sup>+</sup> was assayed not in the thylakoid membrane but with isolated particles in solution [7, 28], a two-component curve was obtained for photoreduction upon a light flash. The fast component reflects reduction of P700<sup>+</sup> by Pc within their complex, while the slow component corresponds to diffusion and binding of free reduced Pc to P700.

We built a corresponding multiparticle model for Pc and PSI (P700) distributed homogeneously in a cubic volume (Fig. 5). The docking probabilities for different redox states and the characteristic life times of complexes as well as the times of electron transfer were calculated from the constants determined experimentally [28] (for Chl *a/b* = 10) and are summarized in the table.

Thereby we modeled the experimental situation described in [28] including all steps of the process (complexing of PC and P700 in either state, direct and back electron transfer, and dissociation of complexes). The cube edge was 1 μm; initial [Pc<sup>I</sup>] = 10 μM (all reduced), [P700<sup>+</sup>] = 0.1 μM (all oxidized); *r* = 4 nm, *D*<sub>Pc</sub> = 10<sup>-10</sup> m<sup>2</sup>/s; integration step, 10 ns. After 500 μs of dark conditions whereby the concentration of the Pc–P700 complex reached a steady state, a flash of light was modeled, converting all reduced P700 to P700<sup>+</sup>. The model kinetic curve for P700<sup>+</sup> reduction after the flash is shown in Fig. 6.

This curve was represented as a sum of two decaying exponentials; knowing their parameters, we approximately calculated the kinetic constants and the times of the Pc–P700 reaction. The values thus obtained were very close to the experimental data for Chl *a/b* = 10 [28].

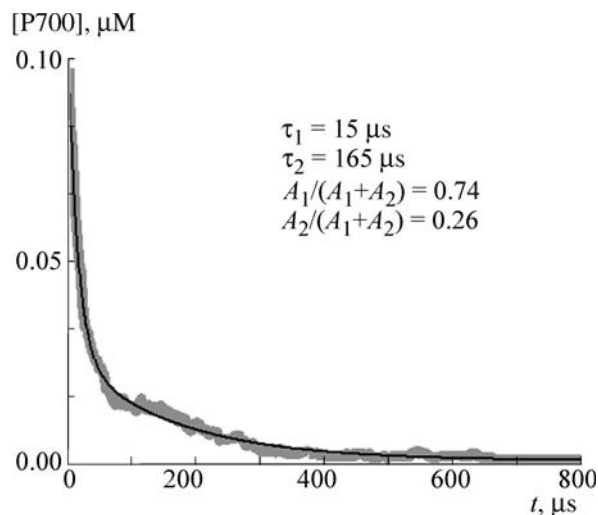


**Fig. 6.** Broad gray line, P700<sup>+</sup> reduction upon a light flash in the direct model (parameters in text). Thin black line, biexponential fitting  $A(t) = A_1 \exp(-t/\tau_1) + A_2 \exp(-t/\tau_2)$ , where  $A_1, A_2$  are amplitudes and  $\tau_1, \tau_2$  are characteristic times of the fast and slow components.

#### CYCLIC ELECTRON TRANSPORT AROUND PHOTOSYSTEM I IN THE MULTIPARTICLE MODEL

Thus, we have shown that the multiparticle model works successfully for proteins in solution. It is still more interesting to test it in a situation when the geometry of the system, the nonuniformity of complex distribution are essential, and the conventional kinetic description is inadequate.

Quite often the experiment deals with multistep kinetics where the characteristic times of the slow components are much longer than those of the elementary reactions. In the kinetic models, such slow components cannot be described without additional assumptions on the organization of the system. It will be shown below that the slow components may be associated with diffusion of the reagents, which is often rate-limiting.

Isolated chloroplasts have been used [21, 30] to study the kinetics of the photoinduced EPR I signal (reflecting the redox state of P700 in the course of cyclic electron transport around PSI) at varied concentrations of exogenous Fd. To exclude electron transfer to oxygen, measurements were performed anaerobically; the pool of reduced Fd required for CET was established by illuminating thylakoids with intense white light for 30 s; 10 μM diuron was added to prevent electron supply from PSII. Light on caused a

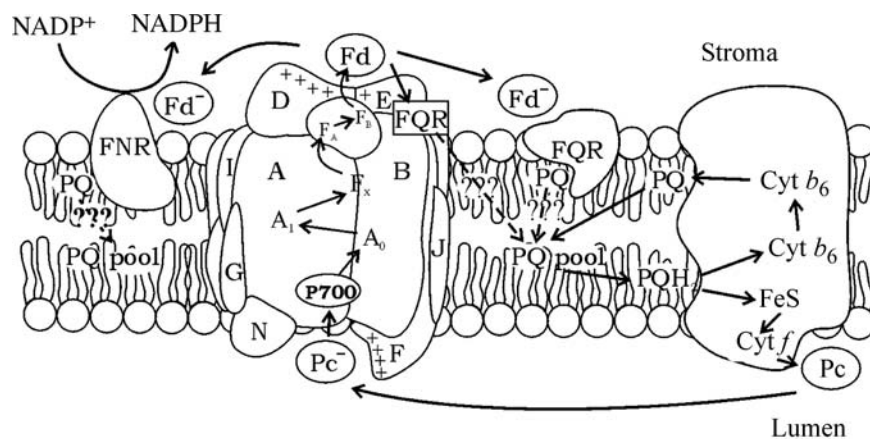


Fig. 7. Scheme of cyclic electron transport in the chloroplast. Question marks denote unknown transfer mechanisms.

rapid rise in EPR I (P700 oxidation) to a steady-state; the kinetics of its reduction with light off was nicely approximated with two exponentials. The characteristic time of the fast phase (0.2 s) was on the same order of magnitude as that for electron transfer from PQ to the Rieske factor of the cytochrome complex. The slow phase (several seconds) exceeded all elementary steps in CET, and was supposed [29] to represent “postreduction” of the strong oxidant P700 by non-specific donors of obscure origin. However, our modeling can explain these phenomena without drawing in such additional vague assumptions.

The CET scheme is outlined in Fig. 7.

Under light, PSI catalyzes Pc oxidation at the luminal side of the thylakoid membrane and Fd reduction at the stromal side; subsequent Fd oxidation and PQ reduction make a segment not coincident with the linear transport. Since Fd is in the aqueous stroma while the hydrophobic PQ is embedded in the lipid layer, this process is likely to involve a membrane stroma-exposed protein with ferredoxin:quinone oxidoreductase activity. Then, PQ oxidation entails reduction of luminal Pc via the *bf* complex in accordance with the Q cycle.

Having estimated the model parameters similarly to those for PC-PSI in solution, we substituted them into the CET model comprising the step shown

by arrows in Fig. 7. In the model we followed the kinetics of dark reduction of P700<sup>+</sup> by Pc. The latter accepts electrons from cyt *f*, which in its turn is reduced at the expense of PQ and Fd. The stage of electron transfer from Fd through PQ to the cytochrome has a characteristic time of about 200 ms (Fig. 8), far longer than that for *f*-Pc-P700<sup>+</sup>. Therefore, in this system the “fast phase” is much slower than in the homogeneous case above when all electrons were initially on Pc (0.2 ms, Fig. 6).

Constructing the stage for multiparticle modeling (Fig. 1), we took into account that PSI is localized in the stromal region of the thylakoid membrane while the cytochrome complexes are spread uniformly through granal and stromal regions. Brownian diffusion of PQ in the membrane and Pc in the lumen was taken to be the same in the two regions. Carrier sizes and concentrations were set in accordance with the literature data; docking times were estimated from the corresponding rate constants. At the initial moment, electrons were distributed over P700, Pc, and partly PQ. In the numerical experiment, after saturating illumination for 1.5 s, we followed the kinetics of P700<sup>+</sup> dark reduction.

Illumination caused reduction of the PQ pool and oxidation of PC and P700, and its time sufficed for uniform distribution of reduced PQ in the stromal

Direct model parameters for Pc-P700 interaction ( $p$  is probability,  $\tau$  is characteristic time,  $\mu$ s)

| $p_{\text{on}}^{\text{I}}$ | $p_{\text{on}}^{\text{I,+}}$ | $p_{\text{on}}^{\text{II}}$ | $p_{\text{on}}^{\text{II,+}}$ | $\tau_{\text{off}}^{\text{I}}$ | $\tau_{\text{off}}^{\text{I,+}}$ | $\tau_{\text{off}}^{\text{II}}$ | $\tau_{\text{off}}^{\text{II,+}}$ | $\tau_{\text{et}}$ | $\tau_{\text{bet}}$ |
|----------------------------|------------------------------|-----------------------------|-------------------------------|--------------------------------|----------------------------------|---------------------------------|-----------------------------------|--------------------|---------------------|
| 0.09                       | 0.09                         | 0.009                       | 0.009                         | 420                            | 420                              | 150                             | 90                                | 17                 | 220                 |

Note: Superscripts (I) and (II) mark reduced and oxidized Pc, (+) denotes oxidized P700; subscripts correspond to (on) formation and (off) dissociation of complex; (et) and (bet) denote direct and back electron transport.

and granal regions of the membrane. After switching off the light, PQ electrons were fed to Pc through the cytochrome complex in both membrane regions (as *bf* is spread uniformly). In the stromal region, Pc<sup>-</sup> fairly quickly reduces P700, because the PSI-*bf* distance there is only some 20 nm [5]; this event corresponds to the fast phase. Both in the experiment and in the model, the fast reduction is incomplete and there remains a fraction of P700<sup>+</sup>; the model shows that this is so because a fraction of electrons is on PQ and PC in the granal region devoid of PSI. These equivalents diffuse into the stromal region to further reduce P700<sup>+</sup>; the time of this phase is determined by the membrane size and geometry, and amounts to 1–10 s. Hence, it is the spatial heterogeneity of the system that determines the biexponential behavior; note that multiparticle modeling obviates assumptions of some nonspecific donor/acceptor pools.

The contribution of the fast component depends on the concentration of added Fd ([30], see above). An increase of the overall amount of electrons in the system augments the amplitude of the fast response but does not influence its rate, determined by the elementary rates in CET which remain the same.

Thus, the kinetics of dark reduction of P700<sup>+</sup> is determined not only by the concentration and redox state of the reagents, but also by their spatial distribution, the geometry and dimensions of the system, and the diffusion features of mobile carriers. Our multiparticle modeling demonstrates that the slow phase in the overall process is controlled by diffusion of reduced PQ and Pc from the granal to the stromal region of the thylakoid membrane, whereas the fast phase is the CET proper involving Fd.

These results are in accord with the fact that in the dark Pc tends to the stromal regions, intergranal thylakoids, and upon illumination migrates laterally into the granal regions [5].

## CONCLUSIONS

The classical (kinetic) approach to modeling the photosynthetic electron and ion transport relies on sets of ordinary differential equations. This may be justified in considering the interactions of isolated fragments with exogenous donors or acceptors in a relatively homogeneous system. However, the lamellar arrangement of the chloroplast is a compartmental, essentially heterogeneous system with nonuniform

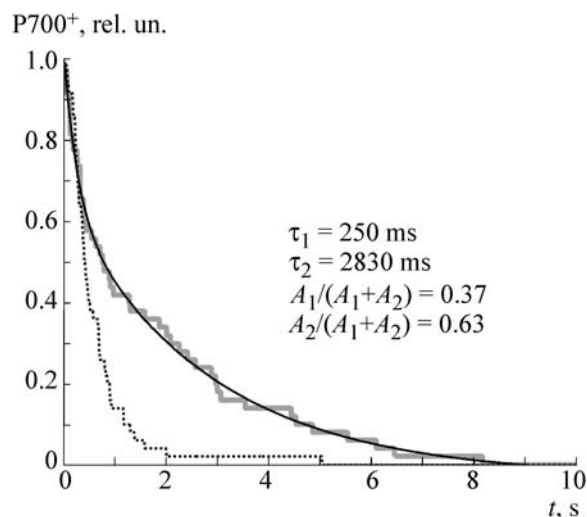


**Fig. 8.** Thick line, P700 reduction curve for the case of two membrane regions differing in complex distribution in accordance with EM data; thin line, its biexponential fitting as in Fig. 6. Dashed line, the curve obtained assuming uniform distribution of complexes through the membrane.

distribution of membrane complexes and diffusion bottlenecks for mobile carriers.

The spatial structure of the membrane can be described with multiparticle computer modeling. This approach can reproduce such specific features as the local inhomogeneity of the system and restricted diffusion of carriers. Here we accounted for lateral heterogeneity but did not explicitly account for the shape of the interacting proteins or electrostatic interactions. These aspects of Pc-*f* interaction in solution have been covered by us previously [24]. We plan to build a model of electron transport by Pc in the lumen that would, on the one hand, consider the intricate geometry of the luminal space and the heterogeneous distribution of membrane complexes, and on the other hand, describe in detail the electrostatics and the protein shape.

## REFERENCES

1. P.-O. Arvidsson and C. Sundby, *Aust. J. Plant Physiol.* **26**, 687 (1999).
2. A. T. Mokronosov and V. F. Gavrilenko, *Photosynthesis: Physiological, Ecological, and Biochemical Aspects* (MGU, Moscow, 1992) [in Russian].
3. A. B. Hope, *Biochim. Biophys. Acta* **1143**, 1 (1993).

4. E. L. Gross, in *Oxygenic photosynthesis: the light reactions*, Ed. by D. R. Ort, C. F. Yocum (Kluwer Academic Publishers, Dordrecht, 1996). Vol. 4, pp. 413–429.
5. W. Haehnel, R. Ratajczak, and H. Robenek, *J. Cell Biol.* **108**, 1397 (1989).
6. M. Mehta, V. Sarafis, and C. Critchley, *Aust. J. Plant Physiol.* **26**, 709 (1999).
7. A. B. Hope, *Biochim. Biophys. Acta.* **1456**, 5 (2000).
8. P.-A. Albertsson, *TRENDS in Plant Science* 6 (8), 349 (2001).
9. H. Kirchhoff, S. Horstmann, and E. Weis, *Biochim. Biophys. Acta* **1459**, 148 (2000).
10. H. Kirchhoff, U. Mukherjee, and H.-J. Galla, *Biochemistry* **41**, 4872 (2002).
11. G. Yu. Riznichenko, *Mathematical Models of Primary Photosynthetic Processes* (VINITI, 1991), Vol. 31 [in Russian].
12. A. Stirbet, Govindjee, B. J. Strasser, and R. J. Strasser, *J. Theor. Biol.* **193**, 131 (1998).
13. G. V. Lebedeva, N. E. Belyaeva, G. Yu. Riznichenko, A. B. Rubin, and O. V. Demin, *Zh. Fiz. Khim.* **74**, 1874 (2000).
14. G. V. Lebedeva, N. E. Belyaeva, O. V. Demin, G. Yu. Riznichenko, and A. B. Rubin, *Biofizika* **47**, 1044 (2002).
15. A. V. Vershubskii, V. I. Priklonskii, and A. N. Tikhonov, *Biofizika* **46**, 471 (2001).
16. G. M. Ullmann, E.-W. Knapp, and N. M. Kostic, *J. Am. Chem. Soc.* **119**, 42 (1997).
17. D. C. Pearson, Jr. and E. L. Gross, *Biophys. J.* **75**, 2698 (1998).
18. M. Ubbink, M. Ejdebeck, B. G. Karlsson, and D. S. Bendall, *Structure* **6**, 323 (1998).
19. F. Rienzo, R. Gabdoulline, M. Menziani, et al., *Biophys. J.* **81**, 3090 (2001).
20. E. L. Gross and D. C. Pearson, Jr., *Biophys. J.* **85**, 2055 (2003).
21. I. B. Kovalenko, D. M. Ustinin, N. E. Grachev, T. E. Krendeleva, G. P. Kukarskikh, K. N. Timofeev, G. Yu. Riznichenko, and A. B. Rubin, *Biofizika* **48**, 656 (2003).
22. I. B. Kovalenko, D. M. Ustinin, N. E. Grachev, E. A. Grachev, and G. Yu. Riznichenko, *Matem. Komput. Obraz.* **3**, 243 (2003).
23. I. B. Kovalenko, D. M. Ustinin, M. V. Serdobol'skaya, N. E. Grachev, and E. A. Grachev, *Proc. VIII Internat. Conf. Nonlinear World* (Fakel, Astrakhan, 2004), pp.223–229.
24. I. B. Kovalenko, A. M. Abaturova, P. A. Gromov, et al., *Phys. Biol.* **3**, 121 (2006).
25. A. Einstein and M. Smoluchowski, *Brownian Motion* (ONTI, Leningrad, 1934) [in Russian].
26. A. B. Rubin, *Biophysics* (KD Universitet, Moscow, 2000) [in Russian].
27. W. Haehnel, T. Jansen, K. Gause, et al., *EMBO J.* **13**, 1028 (1994).
28. F. Drepper, M. Hippler, W. Nitschke, and W. Haehnel, *Biochemistry* **35**, 1282 (1996).
29. H. V. Scheller, *Plant Physiol.* **110**, 187 (1996).
30. T. E. Krendeleva, G. P. Kukarskikh, K. N. Timofeev, B. N. Ivanov, and A. B. Rubin, *Dokl. Akad. Nauk* **379**(5), 1 (2001).